Acta Crystallographica Section D
**Biological Crystallography**
ISSN 0907-4449

# Deleting two C-terminal $\alpha$-helices is effective to crystallize the bacterial ABC transporter *Escherichia coli* MsbA complexed with AMP-PNP

**Kanako Terakado,[a,b] Atsushi Kodan,[b,c] Hiroaki Nakano,[a] Yasuhisa Kimura,[b,d] Kazumitsu Ueda,[c,d] Toru Nakatsu[a,b] and Hiroaki Kato[a,b]***

[a]Department of Structural Biology, Graduate School of Pharmaceutical Sciences, Kyoto University, Kyoto 606-8501, Japan, [b]RIKEN Harima Institute at SPring-8, 1-1-1 Kouto, Sayo-cho, Sayo-gun, Hyogo 679-5148, Japan, [c]Institute for Integrated Cell-Material Sciences, Kyoto University, Kyoto 606-8502, Japan, and [d]Laboratory of Cellular Biochemistry, Division of Applied Life Sciences, Graduate School of Agriculture, Kyoto University, Kyoto 606-8502, Japan

Correspondence e-mail: katohiro@pharm.kyoto-u.ac.jp

Received 12 June 2009
Accepted 27 December 2009



An MsbA deletion mutant ΔC21 that lacks the two C-terminal $\alpha$-helices was expressed in *Escherichia coli* strain C41 and purified by metal-affinity and gel-filtration chromatography. Purified ΔC21 retained 26% of the activity of the wild-type ATPase and had a similar binding affinity to fluorescent nucleotide derivatives. Although crystals of wild-type MsbA complexed with adenosine 5′-($\beta$,$\gamma$-imido)triphosphate could not be obtained, crystals of ΔC21 that diffracted to 4.5 Å resolution were obtained. The preliminary ΔC21 structure had the outward-facing conformation, in contrast to the previously reported *E. coli* MsbA structure. This result suggests that deletion of the C-terminal $\alpha$-helices may play a role in facilitating the outward-facing nucleotide-bound crystal structure of EcMsbA.

## 1. Introduction

ATP-binding cassette (ABC) transporters are a diverse group of prokaryotic and eukaryotic integral membrane proteins that transport a wide variety of chemical compounds across membranes using energy derived from ATP hydrolysis (Holland *et al.*, 2003; Davidson & Chen, 2004). The functional unit of the ABC transporter is composed of two transmembrane domains (TMDs) and two nucleotide-binding domains (NBDs). In bacteria, ABC exporters extrude various substrates, including lipids and drugs, whereas ABC importers mediate the uptake of essential nutrients. MsbA is a bacterial ABC exporter that transports lipid A from the cytoplasmic to the periplasmic side of the inner membrane (Wang *et al.*, 2004; Doerrler *et al.*, 2001, 2004; Doerrler & Raetz, 2002; Zhou *et al.*, 1998). MsbA exists as a dimer consisting of two half-sized subunits that each contain one TMD and one NBD. The amino-acid sequence of MsbA has 30% identity to that of the N-terminal half of P-glycoprotein (Karow & Georgopoulos, 1993) and these proteins share several drugs as transport substrates (Woebking *et al.*, 2005; Eckford & Sharom, 2008). Human P-glycoprotein modulates the pharmacodynamics of drugs and contributes to the multidrug resistance of cancer cells (Chen *et al.*, 1986; Ueda *et al.*, 1987; Gottesman & Pastan, 1993; Gottesman *et al.*, 1996). In a recent report, the X-ray crystal structure of mouse P-glycoprotein was determined at 3.8 Å resolution (Aller *et al.*, 2009).

To date, the X-ray crystal structures of several bacterial ABC exporters have been determined, including those of Sav1866 from *Staphylococcus aureus* at 3.0 Å resolution and MsbA from *Escherichia coli*, *Vibrio cholerae* and *Salmonella typhimurium* (EcMsbA, VcMsbA and StMsbA) at 5.3, 5.5 and 3.7 Å resolution, respectively (Dawson & Locher, 2006; Ward *et al.*, 2007). These structures and electron-microscopy structures (∼20 Å resolution) of MsbA (Ward *et al.*, 2009) suggested that nucleotide binding would cause an intramolecular packing rearrangement of the transmembrane helices and alter the accessibility of the transporter from the cytoplasmic (inward) facing orientation to the periplasmic (outward) facing orientation. The alternating-access model proposes that the transporter has at least two different conformational states, each of which is accessible from only one side of the membrane (Jardetzky, 1966; Tanford, 1983). P-glycoprotein has been crystallized in an inward-facing conformation with and without cyclic hexapeptide inhibitors

(Aller *et al.*, 2009). The structure of non-ligand-bound EcMsbA, which was only solved at low resolution (PDB code 3b5w), shows the transmembrane domain as wide open towards the cytoplasm (inward open conformation), whereas the structure of StMsbA was solved as a nucleotide-bound form in an outward-facing conformation (PDB code 3b60) (Ward *et al.*, 2007). To improve the crystal quality of EcMsbA, we tried to cocrystallize it with many ligands, nucleotides and their derivatives, but were unable to obtain any crystals of the nucleotide-bound form (data not shown). Based on our crystallization attempts, we hypothesized that there might be a structural factor (or issue) that makes it difficult for EcMsbA to maintain the outward-facing conformation in the crystalline state, even with the addition of nucleotides. After examining the EcMsbA structure, we focused on a unique intermolecular interaction between two C-terminal $\alpha$-helices in the crystal (Fig. 1*a*). For example, the two C-terminal $\alpha$-helices of subunits *A*1 and *B*1 (shown in blue and yellow in Fig. 1*a*) in the NBD interact with each other. This type of interaction appeared in all eight subunits in the asymmetric unit. In contrast, the crystal structure of StMsbA in the outward-facing conformation contained no such contacts between the C-terminal $\alpha$-helices (Ward *et al.*, 2007). Moreover, a comparison of the amino-acid sequences of EcMsbA and StMsbA indicated that the C-terminal $\alpha$-helical region from Asn563 to Arg569 has low sequence identity (Fig. 1*b*), despite the high overall sequence identity (96.4%) with only sparsely dispersed nonconserved residues in the entire sequence. Consequently, we propose that deleting the C-terminal $\alpha$-helices would alter the intermolecular interactions between the nucleotide-complexed EcMsbA molecules and promote the growth of another crystal form with an outward-facing conformation.

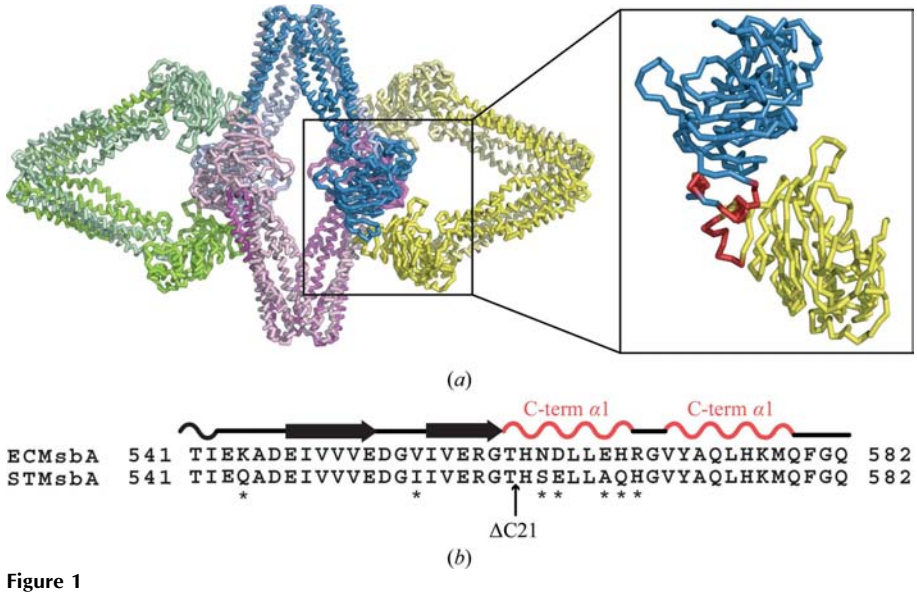


**Figure 1**
Interactions in the EcMsbA crystal and an alignment of the C-terminal amino acids of EcMsbA and StMsbA. (*a*) Four molecules corresponding to an asymmetric unit of EcMsbA (Ward *et al.*, 2007; PDB code 3b5w). Each monomer is represented with subunit *A*1 in blue, subunit *A*2 in pale blue, subunit *B*1 in magenta, subunit *B*2 in pale pink, subunit *C*1 in green, subunit *C*2 in pale green, subunit *D*1 in pale yellow and subunit *D*2 in yellow. The NBDs of subunits *A*1 and *D*2 are enlarged (right). The two C-terminal $\alpha$-helices are indicated in red. (*b*) Sequence alignment of the C-terminal amino acids of EcMsbA and StMsbA with different amino acids highlighted by asterisks. $\alpha$-Helices are shown as wavy lines and $\beta$-sheets as arrows.

Such protein-engineering approaches have been shown to be an effective way of modifying the crystal-packing arrangement and improving crystal quality (Lawson *et al.*, 1991; McElroy *et al.*, 1992; Dyda *et al.*, 1994; Abramson *et al.*, 2003; Chen *et al.*, 1998). In the present study, we report the functional aspects of the EcMsbA ΔC21 deletion mutant as well as a preliminary crystallographic analysis. Deleting the two C-terminal $\alpha$-helices altered the crystal-packing arrangement of EcMsbA complexed with adenosine 5′-($\beta$,$\gamma$-imido-triphosphate (AMP-PNP) and generated an altered structural state with an outward-facing conformation.

## 2. Methods

### 2.1. Plasmid construction

The EcMsbA gene was amplified from *E. coli* W3110 genomic DNA by polymerase chain reaction and was inserted using the *Nde*I/*Bam*HI restriction sites into the pET15b vector with an N-terminal hexahistidine tag and thrombin cleavage site. The EcMsbA mutant lacking 21 C-terminal amino acids (ΔC21) was generated by substituting a termination codon for His562 using the QuikChange site-directed mutagenesis kit (Stratagene) with oligonucleotides 5′-GTGGAACGCGGTACGTAAAACGATTTGCTTGAG-3′ and 5′-CTCAAGCAAATCGTTTTACGTACCGCGTTCCAC-3′.

### 2.2. Expression and purification

Full-length and ΔC21 EcMsbA were cloned into pET15b and transformed into *E. coli* strain C41 (DE3). Protein expression was induced by the addition of 0.2 m*M* isopropyl $\beta$-D-1-thiogalactopyranoside at 310 K for 4 h. The recovered cells were resuspended in 20 m*M* Tris–HCl pH 8.0, 300 m*M* NaCl, 10 m*M* imidazole and 1 m*M* PMSF, disrupted by sonication (Branson 50% duty cycle) and then centrifuged to obtain the soluble fraction. The cell lysates were solubilized with 1%(*w*/*v*) *n*-undecyl $\beta$-D-maltopyranoside ($\beta$-UDM; Anatrace), ultracentrifuged at 100 000*g* for 45 min to remove insoluble materials and then loaded onto a Talon Superflow resin (Clontech). EcMsbA was eluted with 20 m*M* Tris–HCl pH 8.0, 300 m*M* NaCl, 300 m*M* imidazole and 0.02%(*w*/*v*) *n*-undecyl $\beta$-D-thiomaltopyranoside ($\beta$-UTDM; Anatrace). Fractions containing EcMsbA were desalted by dialysis and digested with thrombin (Ito Lifescience). The flowthrough fraction from a Talon Superflow resin was separated on a HiLoad Superdex200 16/60 gel-filtration column (GE Healthcare) with a running buffer consisting of 20 m*M* Tris–HCl pH 8.0, 150 m*M* NaCl and 0.02%(*w*/*v*) $\beta$-UTDM.

### 2.3. Measurement of ATPase activity and determination of TNP-nucleotide binding affinity

The ATPase activity of EcMsbA was determined by measuring the release of inorganic phosphate using the colourimetric method (Chifflet *et al.*, 1988). The nucleotide binding of EcMsbA was measured by fluorescent titration experiments using 2′,3′-*O*-(2,4,6-trinitrophenyl)adenosine 5′-triphosphate (TNP-ATP) and 2′,3′-*O*-(2,4,6-trinitrophenyl)adenosine 5′-diphosphate (TNP-ADP) (Sigma–Aldrich). The fluorescent intensity was measured at 408 nm excitation and 535 nm emission. The dissociation constant $K_d$ was determined using the equation

$$\Delta F = \frac{\Delta F_{\max} \times [\text{TNP-nucleotide}]}{K_d + [\text{TNP-nucleotide}]}. \quad (1)$$

### 2.4. Crystallization, data collection and molecular replacement

Purified EcMsbA ΔC21 was concentrated to 7 mg ml$^{-1}$. The crystals were grown in the presence of 2 m*M* AMP-PNP (Sigma–Aldrich), 6 m*M* $MgCl_2$ and 2.5% 1,2,3-heptanetriol (Fluka) by vapour diffusion in sitting drops at 288 K against a reservoir containing 21.5%(*w*/*v*) polyethylene glycol 400, 0.1 *M* Tris–HCl pH 7.5 and 0.1 *M* sodium formate. Protein crystals appeared after 3–5 d and matured to full size within two weeks. The crystals were cryoprotected in 30%(*w*/*v*) polyethylene glycol 400 and 7.5%(*w*/*v*) glycerol before flash-freezing in liquid nitrogen. X-ray diffraction data were collected at 100 K on BL41XU at SPring-8 with a CCD detector MX225HE (Rayonix). The structure was solved using the molecular-replacement method with the *MOLREP* program (Vagin & Teplyakov, 2000) from the *CCP*4 suite (Collaborative Computational Project, Number 4, 1994). *REFMAC*5 (Murshudov *et al.*, 1997) was used for rigid-body refinement of the model structure. Molecular-graphics figures were created using *PyMOL* (http://www.pymol.org/).

## 3. Results and discussion

The EcMsbA mutant ΔC21, which lacks 21 C-terminal amino acids located in the region of two α-helices, was expressed in *E. coli* strain C41 and purified by metal-affinity and gel-filtration chromatography. The functional properties of EcMsbA ΔC21 were compared with those of full-length EcMsbA. The $k_0$ and $K_m$ for the ATPase activity of ΔC21 decreased to 26.0% and 27.3% of the values for the full-length enzyme, respectively (Table 1). Consequently, the $k_0/K_m$ value changed very little (Table 1). Moreover, ΔC21 had a similar binding affinity for TNP-ATP and TNP-ADP based on fluorescence measurements (Table 1). These data suggest that a considerable amount of ATPase activity is retained by the deletion mutant. Therefore, the ΔC21 mutant appears to preserve its functional structure.

We obtained a crystal of ΔC21 complexed with AMP-PNP that diffracted to 4.5 Å resolution (Fig. 2). The crystallographic data are summarized in Table 2. The preliminary crystal structure was solved by molecular replacement using *MOLREP* and a polyalanine model derived from StMsbA (PDB code 3b60; Ward *et al.*, 2007) that did not include the C-terminal 21 residues of chains *A* and *B* as a starting model. Molecular-replacement calculations yielded a single solution with a correlation coefficient of 70.9 and an *R* factor of 50.8% for data in the resolution range 50–4.5 Å. The *R* and $R_{free}$ factors of the rigid-body refinement model were 37.5% and 39.9%, respectively. The resulting $2F_o - F_c$ map is shown in Fig. 3.

The preliminary structure of EcMsbA ΔC21 was in the outward-facing conformation, similar to the structures of StMsbA with AMP-

**Table 1**
Kinetic parameters of EcMsbA and the affinity of TNP-nucleotides for EcMsbA.

| | Kinetic parameters of ATPase | | | TNP-ATP | TNP-ADP |
|---|---|---|---|---|---|
| | $K_m$ (μ*M*) | $k_0$ (s$^{-1}$) | $k_0/K_m$ (μ*M*$^{-1}$ s$^{-1}$) | $K_d$ (μ*M*) | $K_d$ (μ*M*) |
| Full length | 366 ± 73 | 2.84 ± 0.16 | 7.76 ± 0.43 | 3.48 ± 1.01 | 10.65 ± 2.75 |
| ΔC21 | 100 ± 19 | 0.74 ± 0.03 | 7.40 ± 0.30 | 10.70 ± 1.46 | 15.37 ± 3.83 |

**Table 2**
Data-collection statistics for EcMsbA ΔC21.

Values in parentheses are for the last resolution shell.

| | |
|---|---|
| Space group | *P*1 |
| Unit-cell parameters (Å, °) | *a* = 111.0, *b* = 145.7, *c* = 156.7, α = 67.0, β = 70.6, γ = 70.7 |
| Resolution range (Å) | 49.93–4.50 (4.66–4.50) |
| Total No. of reflections | 94908 |
| No. of unique reflections | 48195 |
| Average redundancy | 1.97 (1.97) |
| Completeness (%) | 98.1 (98.8) |
| $R_{merge}$† | 0.063 (0.339) |
| Reduced $\chi^2$ | 0.97 (1.00) |
| Output $\langle I/\sigma(I)\rangle$ | 8.0 (1.8) |
| Rigid-body refinement | |
| No. of reflections | 45757 |
| *R* (%) | 37.5 |
| $R_{free}$ (%) | 39.9 |

† $R_{merge} = \sum_{hkl}\sum_i |I_i(hkl) - \langle I(hkl)\rangle| / \sum_{hkl}\sum_i I_i(hkl)$.

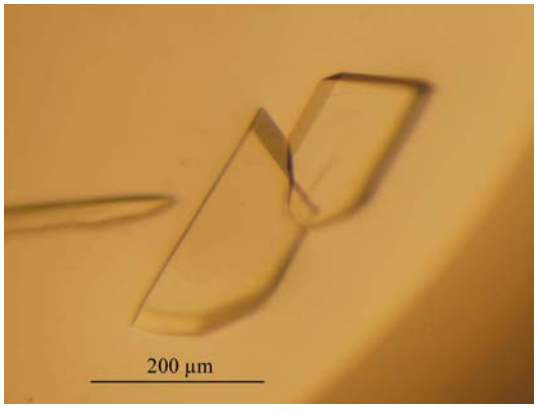


**Figure 2**
Crystals of EcMsbA ΔC21. The scale bar represents 200 μm.

**Figure 3**
$2F_o - F_c$ electron-density map contoured at 1.0σ using the phases obtained from molecular replacement. A $C^\alpha$-trace model (blue) is superposed.

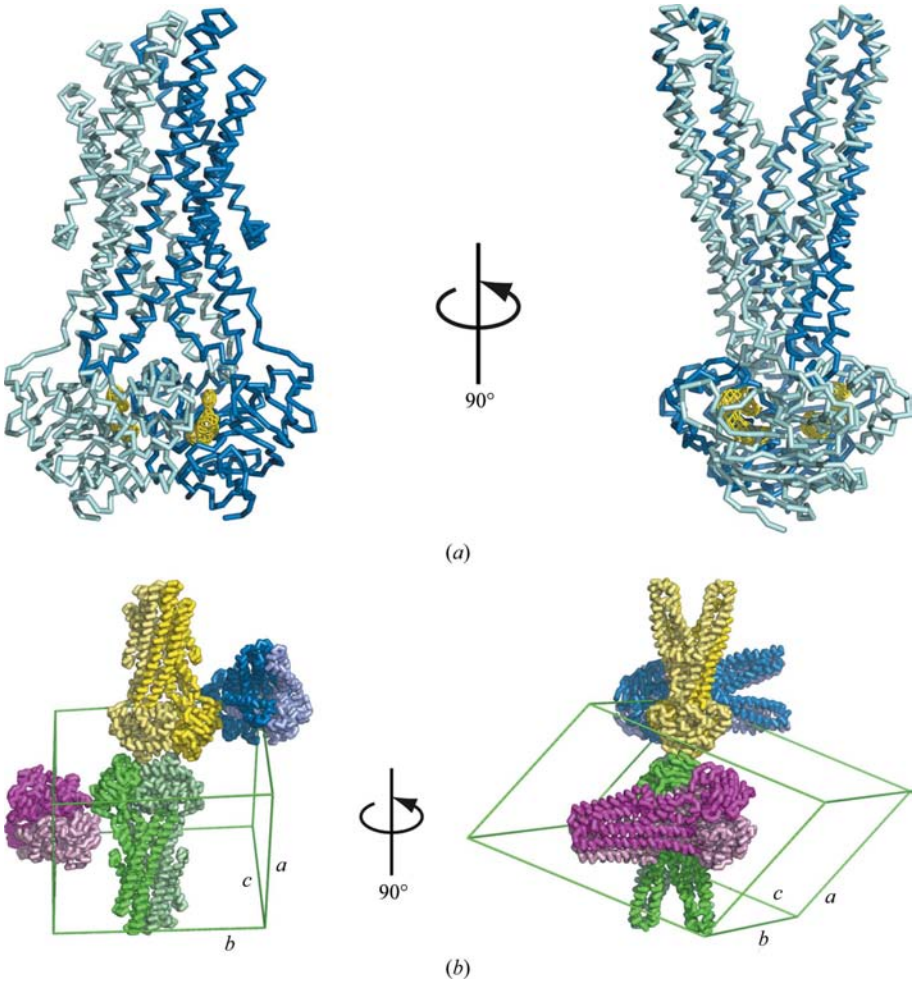


**Figure 4**
Crystal structure and crystal packing of EcMsbA ΔC21. (*a*) $C^{\alpha}$ traces of EcMsbA ΔC21 in two orientations that are rotated by 90° around a vertical axis. Subunit *A* is shown in blue and subunit *B* in pale blue. The $F_o - F_c$ electron-density map is contoured at 3.0$\sigma$ around the nucleotide-binding site (yellow). (*b*) The crystal packing of EcMsbA ΔC21 and the contacts in the asymmetric unit. The right structure is rotated by 90° around a vertical axis. The four dimers in the asymmetric unit are indicated with dimer *A* subunit *A*1 in blue and subunit *A*2 in pale blue, dimer *B* subunit *B* in yellow and subunit *B*2 in pale yellow, dimer *C* subunit *C*1 in magenta and subunit *C*2 in pale pink and dimer *D* subunit *D*1 in green and subunit *D*2 in pale green. The unit cell is represented by a green box and the unit-cell dimensions are labelled *a*, *b* and *c* (see Table 2).

PNP and of Sav1866 with ADP (Fig. 4*a*; Dawson & Locher, 2006; Ward *et al.*, 2007). Significant electron-density lobes that seemed to correspond to two AMP-PNP molecules were observed at the nucleotide-binding site, although these lobes were rather weak and partly discontinuous (Fig. 4*a*).

The current structural model indicates that the crystal packing was rearranged by deleting the C-terminal α-helices, although both the full-length and ΔC21 crystals belonged to the same space group *P*1 and contained a volume that corresponded to the presence of four dimers in the asymmetric unit (Ward *et al.*, 2007). Fig. 4(*b*) illustrates the arrangement of the four dimers in the crystal asymmetric unit. The central dimer in Fig. 4(*b*), named dimer *D*, is shown in green and pale green. There are three types of interactions between the dimer molecules. Firstly, the C-terminal region of the NBD in subunit *D*2 (pale green) of dimer *D* appears to contact the same region in subunit *B*2 (pale yellow) of dimer *B* (yellow and pale yellow). Secondly, dimer *A* (blue and pale blue) and dimer *B* appear to interact between the connecting loops of the TMD and NBD, around Glu330–Arg337 in subunit *A*1 (blue) and Lys332–Arg337 in subunit *B*1 (yellow). The loop in subunit *A*1 also seems to be adjacent to the NBD region (Arg441–Arg446) of subunit *B*1. Thirdly, dimer *D* and dimer *C* (magenta and pale pink) appear to interact between the NBD region around Glu397 in subunit *D*1 (green) and the NBD region (around Asp467-Asn468) in subunit *C*1 (magenta). The NBD region of subunit *D*1 also seems to be close to the NBD region (Gly353–Val356) of subunit *C*2 (pale pink). Although the periplasmic loop region of the TMD in dimer *D* appears to be adjacent to the same region in dimer *B* of the neighbouring unit cell, this interaction was not observed based on the electron densities.

In this study, we obtained new EcMsbA crystals with a structure in the outward-facing conformation, which differs from the previously reported EcMsbA structure (Ward *et al.*, 2007). We found that deleting unique intermolecular interactions between the two C-terminal α-helices helped to form the outward-facing conformation in the complex with AMP-PNP, similar to StMsbA, and that this conformational change dictated the crystal-packing rearrangement. In addition, we suggest that modifying the crystal-packing arrangement is an effective strategy to obtain structures in new conformational states. Future and ongoing research will further improve the crystal structure resolution and refine the preliminary structural model of EcMsbA ΔC21.

We thank Dr T. Shimizu for technical support during X-ray diffraction data collection and Mr M. Tsuji for cloning of MsbA. This work was supported by a Grant-in-Aid for Scientific Research and the Target Protein Research Program from the Ministry of Education, Culture, Sports, Science and Technology (MEXT) of Japan and by a grant from the Takeda Science Foundation. KT was supported by a grant from the 21st Century COE Program 'Knowledge Information Infrastructure for Genome Science' from MEXT and the Junior Research Associate Program of RIKEN. AK and KU were supported by the World Premier International Research Center Initiative, MEXT.

## References

Abramson, J., Smirnova, I., Kasho, V., Verner, G., Kaback, H. R. & Iwata, S. (2003). *Science*, **301**, 610–615.
Aller, S. G., Yu, J., Ward, A., Weng, Y., Chittaboina, S., Zhuo, R., Harrell, P. M., Trinh, Y. T., Zhang, Q., Urbatsch, I. L. & Chang, G. (2009). *Science*, **323**, 1718–1722.
Chen, C., Chin, J. E., Ueda, K., Clark, D. P., Pastan, I., Gottesman, M. M. & Roninson, I. B. (1986). *Cell*, **47**, 381–389.
Chen, G.-Q., Sun, Y., Jin, R. & Gouaux, E. (1998). *Protein Sci.* **7**, 2623–2630.
Chifflet, S., Torriglia, A., Chiesa, R. & Tolosa, S. (1988). *Anal. Biochem.* **168**, 1–4.
Collaborative Computational Project, Number 4 (1994). *Acta Cryst.* D**50**, 760–763.
Davidson, A. L. & Chen, J. (2004). *Annu. Rev. Biochem.* **73**, 241–268.
Dawson, R. J. & Locher, K. P. (2006). *Nature (London)*, **443**, 180–185.

Doerrler, W. T., Gibbons, H. S. & Raetz, C. R. (2004). *J. Biol. Chem.* **279**, 45102–45109.
Doerrler, W. T. & Raetz, C. R. (2002). *J. Biol. Chem.* **277**, 36697–36705.
Doerrler, W. T., Reedy, M. C. & Raetz, C. R. (2001). *J. Biol. Chem.* **276**, 11461–11464.
Dyda, F., Hickman, A. B., Jenkins, T. M., Engelman, A., Craigie, R. & Davies, D. R. (1994). *Science*, **266**, 1981–1986.
Eckford, P. D. & Sharom, F. J. (2008). *J. Biol. Chem.* **283**, 12840–12850.
Gottesman, M. M. & Pastan, I. (1993). *Annu. Rev. Biochem.* **62**, 385–427.
Gottesman, M. M., Pastan, I. & Ambudkar, S. V. (1996). *Curr. Opin. Genet. Dev.* **6**, 610–617.
Holland, I. B., Cole, S. P. C., Kuchler, K. & Higgins, C. F. (2003). *ABC Proteins: From Bacteria to Man.* London: Academic Press.
Jardetzky, O. (1966). *Nature (London)*, **211**, 969–970.
Karow, M. & Georgopoulos, C. (1993). *Mol. Microbiol.* **7**, 69–79.
Lawson, D. M., Artymiuk, P. J., Yewdall, S. J., Smith, J. M., Livingstone, J. C., Treffry, A., Luzzago, A., Levi, S., Arosio, P., Cesareni, G., Thomas, C. D., Shaw, W. V. & Harrison, P. M. (1991). *Nature (London)*, **349**, 541–544.
McElroy, H. E., Sisson, G. W., Schoettlin, W. E., Aust, R. M. & Villafranca, J. E. (1992). *J. Cryst. Growth*, **122**, 265–272.
Murshudov, G. N., Vagin, A. A. & Dodson, E. J. (1997). *Acta Cryst.* D**53**, 240–255.
Tanford, C. (1983). *Proc. Natl Acad. Sci. USA*, **80**, 3701–3705.
Ueda, K., Cardarelli, C., Gottesman, M. M. & Pastan, I. (1987). *Proc. Natl Acad. Sci. USA*, **84**, 3004–3008.
Vagin, A. & Teplyakov, A. (2000). *Acta Cryst.* D**56**, 1622–1624.
Wang, X., Karbarz, M. J., McGrath, S. C., Cotter, R. J. & Raetz, C. R. (2004). *J. Biol. Chem.* **279**, 49470–49478.
Ward, A., Mulligan, S., Carragher, B., Chang, G. & Milligan, R. A. (2009). *J. Struct. Biol.* **165**, 169–175.
Ward, A., Reyes, C. L., Yu, J., Roth, C. B. & Chang, G. (2007). *Proc. Natl Acad. Sci. USA*, **104**, 19005–19010.
Woebking, B., Reuter, G., Shilling, R. A., Velamakanni, S., Shahi, S., Venter, H., Balakrishnan, L. & van Veen, H. W. (2005). *J. Bacteriol.* **187**, 6363–6369.
Zhou, Z., White, K. A., Polissi, A., Georgopoulos, C. & Raetz, C. R. (1998). *J. Biol. Chem.* **273**, 12466–12475.